Heat transfer Analysis of Magneto-Micropolar Fluid Flow over an Inclined Non-linearly Permeable Stretching Sheet with Variable Fluid Properties

E. O. Fatunmbi[1], A. Adeniyan [2]

[1-2]Department of Mathematics and Statistics, Federal Polytechnic, Ilaro, Nigeria.
E-mail: [1]ephesus.fatunmbi@federalpolyilaro.edu.ng; [2]aadeniyan@unilag.edu.ng
Corresponding author e-mail: ephesus.fatunmbi@federalpolyilaro.edu.ng

Abstract
In this study, an analysis of Magneto-micropolar fluid flow and heat transfer characteristics over an inclined nonlinearly permeable stretching sheet is investigated. The fluid properties such as the dynamic viscosity and thermal conductivity are taken to be temperature dependent while the electrical conductivity vary with the fluid velocity. The influences of non-uniform heat source/sink, variable applied magnetic field with power law surface temperature as the thermal boundary condition are also examined. Appropriate similarity transformation variables are employed to reduce the modelled governing equations into a system of nonlinear ordinary differential equations. Subsequently, Runge-Kutta-Fehlberg integration scheme cum shooting techniques is applied to yield the numerical solutions for the model. The findings are both depicted on graphs and tables for various controlling parameters. In the limiting situations, the results generated compared favourably with the earlier reported data in the literature. The results show that the momentum and thermal boundary layer thicknesses fall with an increase in the nonlinear stretching parameter while the opposite occur with a rise in the thermal conductivity parameter.
Keywords: Micropolar fluid; nonlinear stretching sheet; temperature-dependent properties; inclined sheet

1 Introduction

The study of non-Newtonian fluids has gain prominence due to its practical industrial and diverse applications in engineering processes. Due to great diversity in the physical structure of non-Newtonian fluids, a single constitutive Model cannot captured all, thus various Models exist such as Casson fluids, Jeffery fluids, Maxwell fluids, Micropolar fluids etc. Notable among the non-Newtonians is the micropolar fluid (Eringen, 1966). These are fluids with microstructure. They exhibit certain microscopic effect arising from the local structure and micromotion of the fluid element.

Newtonian fluids cannot effectively describe the complex mechanical behaviour that fluid exhibit at micro level. Micropolar fluid is prominent among others because it offers a good mathematical model for simulating the flow characteristics of polymeric suspensions, colloidal fluids, liquid crystals, animal blood etc.

1.1 Various Applications of this Study

Various application of this study can be seen in engineering and industrial activities. Firstly, the study of transfer over stretching surfaces has gained prominence due to its various industrial applications. A wider range of applications of stretching plates are frequently encountered in extrusion of plastic sheet and metal extrusion, hot rolling, drawing of plastic films paper and textile production, polymer processing industries cooling of electronic devices by fans. Other areas are: manufacturing of plastic and rubber sheet, the cooling of metallic sheets, etc.

1.2 Micropolar Fluids Applications in Engineering

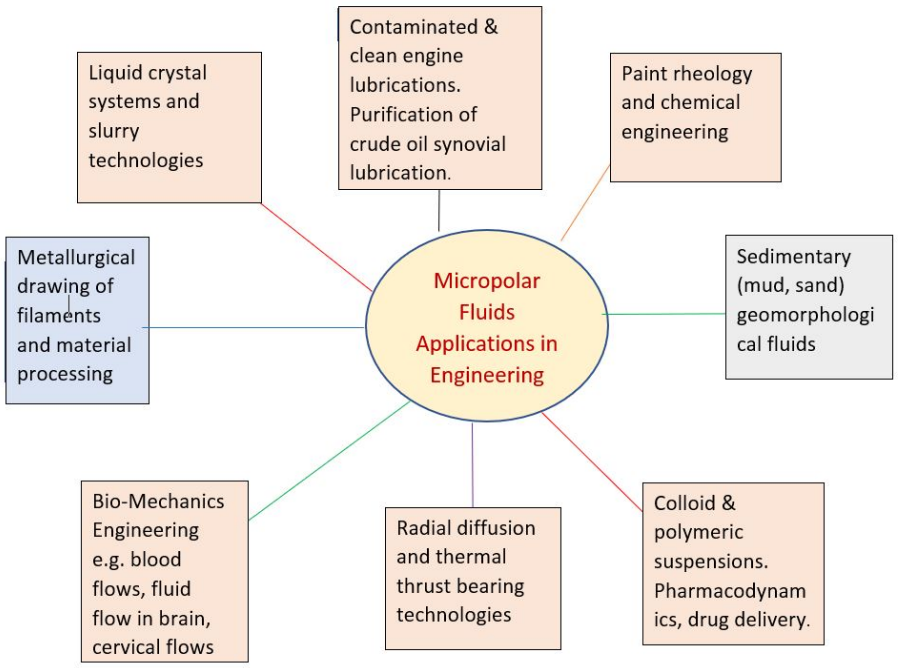

1.3 Review of Literature

Notable authors have worked on stretching sheet with or without variable properties. Authors such as Cortell (2007, 2008); Hayat *et al.* (2008)and Kumar (2009) have researched into the influence of various parameters on the flow of Newtonian fluid over a stretching sheet. Ahmad *et al.*, (2014) investigated MHD micropolar fluid flow on nonlinearly impermeable stretching sheet with constant properties while Salem (2013) studied on MHD micropolar nonlinearly stretching sheet with variable viscosity.

Recently, Fatunmbi and Fenuga (2018) reported on the flow of an electrical conducting non-Newtonian fluid of micropolar type with temperature-dependent material properties. Furthermore, Rahman*et al.*, (2009) examined variable fluid properties on an inclined plate whereas Akinbobola and Okoya (2015) reported on such problem with the flow of visco-elastic fluid on a stretching sheet with variable viscosity. Tripathy *et al.* (2016) as well as Shamshuddin and Thunma (2019) investigated numerical MHD flow of micropolar fluid on stretching fluid with constant properties. In the present work, we studied MHD micropolar fluid flow passing an inclined sheet with variable properties and prescribed temperature.

2 Mathematical Formulation of the Problem

2.1 Basic Assumptions

The following assumptions are considered for the mathematical formulation of the model equations of the fluid flow, microrotation and energy distributions.

- The flow is two-dimensional (x, y), incompressible and steady and the sheet is inclined, permeable and stretching with velocity $u_w = cx^r$.
- The corresponding velocity components are (u, v). The x axis is taken along the direction of flow with y axis normal to it.
- The fluid is electrically conducting Micropolar fluid.with the applied magnetic field being a function of x and normal to the flow direction.
- The dynamic fluid viscosity and thermal conductivity are assumed to be temperature-dependent.
- The magnetic Reynolds number of the flow is taken to be small enough so that the induced magnetic field is negligible and no electric field.

- The electrical conductivity σ is assumed to be a function of u and non-uniform heat source/sink is applied.

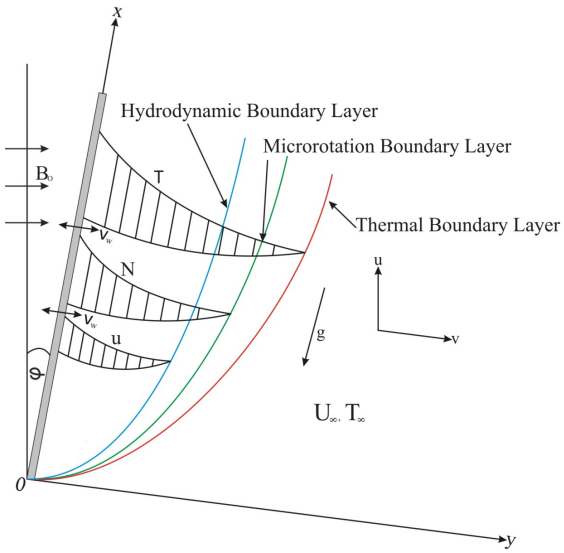

Figure 1. Flow Configuration and the Coordinate System

With the use of Oberbeck-Boussinesq and the boundary approximations, the boundary layer governing equations for the model are given as follow:

$$\frac{\partial u}{\partial x}+\frac{\partial v}{\partial y}=0, \tag{1}$$

$$u\frac{\partial u}{\partial x}+v\frac{\partial u}{\partial y}=\frac{1}{\rho_\infty}\frac{\partial}{\partial y}\left(\mu\frac{\partial u}{\partial y}\right)+\frac{\mu_r}{\rho_\infty}\frac{\partial^2 u}{\partial y^2}+\frac{\mu_r}{\rho_\infty}\frac{\partial N}{\partial y}+g\beta_T\left(T-T_\infty\right)cos\alpha-\frac{\sigma_0'\left(B(x)\right)^2}{\rho_\infty}u \tag{2}$$

$$u\frac{\partial N}{\partial x}+v\frac{\partial N}{\partial y}=\frac{\gamma}{\rho j}\frac{\partial^2 N}{\partial y^2}-\frac{\mu_r}{\rho j}\left(2N+\frac{\partial u}{\partial y}\right), \tag{3}$$

$$u\frac{\partial T}{\partial x}+v\frac{\partial T}{\partial y}=\frac{1}{\rho_\infty c_p}\frac{\partial}{\partial y}\left[\left(\kappa+\frac{16T_\infty^3\sigma^\star}{3k^\star}\right)\frac{\partial T}{\partial y}\right]+\frac{(\mu+\mu_r)}{\rho_\infty c_p}\left(\frac{\partial u}{\partial y}\right)^2+\frac{\sigma_0'\left(B(x)\right)^2}{\rho_\infty c_p}u^2+\frac{q'''}{\rho_\infty c_p}, \tag{4}$$

The suitable boundary conditions are::

$$\begin{aligned}&u=u_w=cx^r, v=v_w, N=-h\frac{\partial u}{\partial y}, T=T_w=\left(Ax^n+T_\infty\right)\quad at\ y=0,\\&u\longrightarrow 0, N\longrightarrow 0, T\longrightarrow T_\infty\quad \text{as}\quad y\to\infty.\end{aligned} \tag{5}$$

The description of the embedded variables are as follows μ, ν, ρ_∞, μ_r, j and γ represent the dynamic viscosity, kinematic viscosity, density of the ambient fluid, vortex viscosity, micro inertial per unit mass and spin gradient viscosity in that order. Also, T, N, κ represent the fluid temperature, component of microrotation vector normal to x, y plane, thermal conductivity respectively.Likewise, the electrical conductivity is taken to be dependent on the fluid velocity as

$$\sigma_0'=\sigma_0 u \tag{6}$$

and the applied magnetic field is a function of x given as (see Rahman, Uddin and Aziz, 2009).

$$B(x)=\frac{B_0}{\sqrt{x}} \tag{7}$$

where σ_0 and B_0 are constants. Similarly, c_p stands for the specific heat at constant pressure while T_∞ indicates the free stream temperature.
The non-uniform heat source/sink is given as

$$q'''=\frac{\kappa u_w}{x^r\nu}\left[A^\star\left(T_w-T_\infty\right)f'+B^\star\left(T-T_\infty\right)\right] \tag{8}$$

where $A^\star$ and $B^\star$ connote the space dependent heat source/sink and $B^\star$ the temperature dependent heat source/sink.
The suction/injection term in equation (5) is symbolized with v_w, it is assumed that $v_w = V_0 x^{(r-1)/2}$, $A^\star = \alpha_1 x^{r-1}$ and $B^\star = \beta_1 x^{r-1}$ where V_0, α_1 and β_1 are constants (see Das al., 2015 and references there-in). Also, h is a surface boundary parameter with $0 \leq h \leq 1$. The case when $h = 0$ corresponds to $N = 0$, this represents a strong concentration such that the micro-particles close to the wall are unable to rotate. The situation of $h = 1/2$ shows that there weak concentration of micro-particles and also indicating the vanishing of anti-symmetric part of the stress tensor while $h = 1$ models turbulent boundary layer situations (see Peddieson, 1972; Ahmadi, 1976; Jena and Mathur, 1981).
The temperature-dependent viscosity $\mu(T)$ can be expressed as (see Das, 2012; Akinbobola & Okoya, 2015 and the cited references).

$$\frac{1}{\mu} = \frac{1}{\mu_\infty}\left[1 + \beta\left(T - T_\infty\right)\right], \tag{9}$$

Equation (9) also implies

$$\frac{1}{\mu} = H\left(T - T_r\right), \tag{10}$$

here, $H = \frac{\beta}{\mu_\infty}$ and $T_r = T_\infty - \frac{1}{\beta}$ are constants, their values are determined by the reference state of the fluid whereas β describes the thermal nature of the micropolar fluid. Other models of temperature-dependent viscosity includes the Vogel's and the Reynolds viscosity model, however, the model in equation (9) is more appropriate for a broad range of temperature than the other models (Knezevic and Savic, 2006; Keimanesh and Aghanajafi, 2017).

Also, Chiam (1996, 1998) reported that for liquid metals, the variation of the thermal conductivity κ with temperature can be expressed in an approximately linear form having the range of $0^o F$ to $400^0 F$. Obviously, this relationship can take the linear form described in equation (10) as

$$\kappa\left(T_w - T_\infty\right) = \kappa_\infty\left[\left(T_w - T_\infty\right) + \delta\left(T - T_\infty\right)\right]. \tag{11}$$

Here, κ_∞ represents the free stream thermal conductivity, δ denotes variable thermal conductivity parameter. Meanwhile, Mahmoud (2012) reported that the range of values of $0 \leq \epsilon \leq 6$ is applicable for air with $0 \leq \epsilon \leq 0.12$ for water while $-0.1 \leq \epsilon \leq 0.12$ for lubrication oils.
By means of equation (12) the modelled equations are transmuted from nonlinear partial differential equations to nonlinear coupled ordinary differential equations η (see Hayat *et al.*, 2008; Salem, 2013)

$$\begin{aligned}
&\eta = y\left[\frac{c(r+1)x^r}{2x\nu_\infty}\right]^{1/2},\ \psi = x^{(r-1)/2}\left[\frac{2c(r+1)}{(r+1)}\right]^{1/2} f(\eta),\ N = x^{(3r-1)/2}\left[\frac{c^3(r+1)}{2\nu_\infty}\right]^{1/2} g(\eta)\\
&u = cx^r f', v = -\left[\frac{c\nu_\infty(r+1)}{2}\right]^{1/2} x^{(r-1)/2}\left(f + \frac{(r-1)}{(r+1)}\eta f'\right),\ \gamma = \left(\mu + \frac{\mu_r}{2}\right) j,\ j = \left(\frac{\nu}{c}\right) x^{(1-r)}\\
&\theta(\eta) = \frac{T - T_\infty}{T_w - T_\infty} \Rightarrow \frac{T - T_r}{T_w - T_\infty} + \theta r,\ \theta r = \frac{T_r - T_\infty}{T_w - T_\infty}.
\end{aligned} \tag{12}$$

With the use of equation (12) in equations (10-11), equation (9) becomes

$$\mu(T) = \left(\frac{\theta r}{\theta r - \theta}\right)\mu_\infty \tag{13}$$

while equation (10) implies

$$\kappa = \kappa_\infty\left(1 + \delta\theta\right)., \tag{14}$$

(see Oahimire & Olajuwon, 2013), meanwhile, the application of the stream function given as

$$u = \frac{\partial\psi}{\partial y}, v = -\frac{\partial\psi}{\partial x}, \tag{15}$$

enhances the satisfaction of the continuity equation (1). Then on substituting equation (12) into equations (2-5) and taking cognizance of equations (6-7) and (13-14) the governing equations result to the underlisted non-linear ordinary differential equations

$$\left(\frac{\theta r}{\theta r - \theta} + K\right) f''' + ff'' + Kg' - \left(\frac{2r}{r+1}\right) f'^2 + \frac{\theta r}{(\theta r - \theta)^2}\theta' f'' + \left(\frac{2}{r+1}\right) Gr\cos\varphi - \left(\frac{2}{r+1}\right) Mf'^2 = 0, \tag{16}$$

$$\left(1 + K/2\right) g'' + fg' - \left(\frac{3r-1}{r+1}\right) f'g - K\left(2g + f''\right)\left(\frac{2}{r+1}\right) = 0, \tag{17}$$

$$(1+\delta\theta+Nr)\,\theta''+\delta\theta'^2+Pr_\infty\left(f\theta'-\frac{2n}{r+1}f'\theta\right)+\left(\frac{\theta r}{\theta r-\theta}+K\right)Pr_\infty Ecf''^2+$$
$$\left(\frac{2}{r+1}\right)Pr_\infty MEcf'^3+\left(\frac{2}{r+1}\right)Pr_\infty\,(1+\delta\theta)\,(\alpha^\star f'+\beta^\star\theta)=0. \tag{18}$$

For a realistic result of the energy equation (18), it is required that the Prandtl number vary across the boundary layer since the definition of the Prandtl number Pr involves both viscosity μ, specific heat capacity and thermal conductivity κ, that is, $Pr=\frac{\mu c_p}{\kappa}$. Hence, by implication of the combined variable viscosity μ as well as thermal conductivity κ, the variable Prandtl number is incorporated (see Rahman *et al.*, 2010). Thus,

$$Pr=\frac{\mu c_p}{\kappa}=\frac{\left(\frac{\theta r}{\theta r-\theta}\right)\mu_\infty c_p}{k_\infty(1+\delta\theta)}=\frac{1}{(1-\frac{\theta}{\theta r})(1+\delta\theta)}Pr_\infty. \tag{19}$$

By making use of equation (19), the energy equation (18) becomes

$$(1+\delta\theta+Nr)\,\theta''+\delta\theta'^2+Pr\left(1-\frac{\theta}{\theta r}\right)(1+\delta\theta)\left[\left(f\theta'-\left(\frac{2n}{r+1}\right)f'\theta\right)\right]+$$
$$Pr\left(1-\frac{\theta}{\theta r}\right)(1+\delta\theta)\left[\left(\frac{\theta r}{\theta r-\theta}\right)+K\right]Ecf''^2+\left(\frac{2}{r+1}\right)Pr\left(1-\frac{\theta}{\theta r}\right)(1+\delta\theta)\,MEcf'^3+ \tag{20}$$
$$\left(\frac{2}{r+1}\right)Pr\left(1-\frac{\theta}{\theta r}\right)(1+\delta\theta)^2\,(\alpha^\star f'+\beta^\star\theta)=0.$$

The transformed boundary conditions are:

$$\begin{aligned}&\eta=0: f'=1,\ f=fw,\ g=-hf'',\ \theta=1,\\ &\eta\longrightarrow\infty: f'=0,\ g\longrightarrow 0,\ \theta\longrightarrow 0.\end{aligned} \tag{21}$$

The nomenclature of the parameters included in equations (16-21) are given as:

$$K=\frac{\mu_r}{\mu_\infty},\ M=\frac{\sigma_0 B_o^2}{\rho},\ Pr=\left[\left(1-\frac{\theta}{\theta r}\right)(1+\epsilon\theta)\right]^{-1}Pr_\infty,$$
$$Pr_\infty=\frac{\mu_\infty c_p}{\kappa_\infty},\ Gr=\frac{g\beta_T\,(T_w-T_\infty)\,x}{u_w^2},\ Ec=\frac{u_w^2}{c_p\,(T_w-T_\infty)},\ \alpha^\star=\frac{\alpha_1\kappa_\infty}{\mu_\infty c_p}, \tag{22}$$
$$\beta^\star=\frac{\beta_1\kappa_\infty}{\mu_\infty c_p},\ fw=\frac{-\sqrt{2}V_0}{\left(\sqrt{c\nu(r+1)}\right)},\ \theta r=\frac{-1}{\beta\,(T_w-T_\infty)}.$$

In the above equations (16-20), the differentiation is carried out with respect to η. Similarly, K is the micropolar material parameter, the suction/injection parameter is represented by fw, where $fw>0$ indicates suction and $fw<0$ corresponds to injection while $fw=0$ depicts an impermeable sheet and M is the Magnetic field parameter. In addition, Pr symbolizes the Prandtl number where Pr_∞ is the ambient Prandtl number, the space and heat dependent heat source/sink are $\alpha^\star$ and $\beta^\star$ respectively, δ symbolizes thermal conductivity variation parameter while Gr is the Grashof number and the Eckert number is represented by Ec, θr stands for the viscosity variation parameter which is dependent on the temperature difference alongside with the viscosity/temperature nature of the fluid.

3 Method of Solution

To get solutions to the highly nonlinear equations (16-18, 20) subject to conditions (21). A computer algebra symbolic Maple 2016 package is employed. The numerical procedure follows Runge-Kutta techniques of fourth order incorporated with a shooting scheme. To check the validity of the the numerical code used, we have compared our results in the limiting condition with that of Cortell (2007) and Hayat (2008) as shown in Table 1 relating to the skin friction coefficient C_{f_x}. Besides, we also crosschecked the values of the Nusselt number Nu_x in the limiting case with those authors used in Table 1, these are recorded in Table 2.

4 Analysis of Results and Discussion

This section includes validation of results, presentation of results in tabular and graphical forms and then the discussion of results.

4.1 Validation of Results

Tables 1 and 2 portray the validation of the present results with the related articles in the literature in some limiting conditions. It is clearly shown that the present results have an excellent relationship with the previously published works as depicted from the Tables.

Table 1: Comparison of values of C_{f_x} with variations in r

r	Cortell	Hayat	Present
00	0.627547	0.627555	0.627563
0.2	0.766758	0.766837	0.766846
0.5	0.889477	0.889544	0.889552
1.0	1.000000	1.000000	1.000008
1.5	1.061587	1.061601	1.061609
3.0	1.148588	1.148593	1.148601
7.0	1.216847	1.216850	1.216858
10.0	1.234875	1.234875	1.234882
20.0	1.257418	1.257424	1.257431
100.0	1.276768	1.276774	1.276781

Table 2: Comparison of the values of Nu_x for Newtonian fluids when $Ec = K = \gamma = j = Gr = Nr = \epsilon = 0, \theta r \to \infty$ with variations in r

Ec	r	Cortell $Pr = 1$	Hayat $Pr = 1$	Present $Pr = 1$	Cortell $Pr = 5$	Hayat $Pr = 5$	Present $Pr = 5$
00	0.2	0.610262	0.610202	0.610216	1.607175	1.607925	1.607784
	0.5	0.595277	0.595201	0.595224	1.586744	1.586833	1.586779
	1.5	0.574537	0.574730	0.574771	1.557463	1.557672	1.557692
	3.0	0.564472	0.564462	0.564717	1.542337	1.542145	1.543178
	10.0	0.554960	0.554878	0.554951	1.528573	1.528857	1.528926

4.2 Tabular Presentation of Results

The reaction of various embedded parameters as regard the skin friction coefficient C_{f_x} and Nusselt number Nu_x afre shown in Tables 3-7.

Table 3: Values of C_{f_x} and Nu_x with variations in r for the case of suction $fw > 0$ and injection $fw < 0$

	VEC	CEC	VEC	CEC	VEC	CEC	VEC	CEC
r	$-f(0)''$	$-f(0)''$	$-\theta'(0)$	$-\theta'(0)$	$-f(0)''$	$-f(0)''$	$-\theta'(0)$	$-\theta'(0)$
		$fw = 0.1$				$fw = -0.1$		
0.2	-0.26179	-0.25479	0.37217	0.35953	-0.28545	-0.58661	0.40307	0.51601
0.6	0.07735	0.11893	0.13733	0.14839	0.04795	0.08125	0.17869	0.18980
1.2	0.19283	0.23752	0.05098	0.06657	0.16188	0.19986	0.09595	0.11208
1.4	0.25058	0.29526	0.00659	0.02351	0.21899	0.25777	0.05328	0.07098
1.6	0.29769	0.34158	-0.03016	-0.01266	0.26567	0.30432	0.01785	0.03632

Table 4: Values of C_{f_x} and Nu_x with variations in K for the case of suction $fw > 0$ and injection $fw < 0$

	VEC	CEC	VEC	CEC	VEC	CEC	VEC	CEC
K	$-f''(0)$	$-f''(0)$	$-\theta'(0)$	$-\theta'(0)$	$-f''(0)$	$-f''(0)$	$-\theta'(0)$	$-\theta'(0)$
		$fw = 0.1$				$fw = -0.1$		
0.0	0.20869	0.25251	0.02511	0.04960	0.17388	0.21002	0.07277	0.09634
1.0	0.20186	0.24691	0.03954	0.05878	0.16866	0.20653	0.08577	0.10492
3.0	0.18527	0.22919	0.06112	0.07409	0.15634	0.19397	0.10492	0.11887
5.0	0.17343	0.21524	0.07842	0.08834	0.14779	0.18407	0.12015	0.13157
7.0	0.16458	0.20403	0.09257	0.10127	0.14148	0.17605	0.13256	0.14294

Table 5: Values of C_{f_x} and Nu_x with variations in θr for the case of suction $fw > 0$ and injection $fw < 0$

	VEC	CEC	VEC	CEC	VEC	CEC	VEC	CEC
θr	$-f''(0)$	$-f''(0)$	$\theta(0)$	$\theta(0)$	$-f''$	$-f''(0)$	$\theta(0)$	$\theta(0)$
	$fw = 0.1$				$fw = -0.1$			
2.5	0.19324	0.23874	0.09386	0.11238	0.15827	0.19597	0.14474	0.16381
3.5	0.19084	0.23646	0.14399	0.16599	0.15165	0.18832	0.20210	0.22473
5.0	0.18776	0.23311	0.18235	0.20706	0.14557	0.18117	0.24624	0.27165
7.0	0.18530	0.23035	0.20828	0.23484	0.14117	0.17595	0.27618	0.30349
10.0	0.18328	0.22806	0.22790	0.25587	0.13773	0.17186	0.29889	0.32767

Table 6: Values of C_{f_x} and Nu_x with variations in φ for the case of suction $fw > 0$ and injection $fw < 0$

	VEC	CEC	VEC	CEC	VEC	CEC	VEC	CEC
φ	$f''(0)$	$f''(0)$	$-\theta'(0)$	$-\theta'(0)$	$f''(0)$	$f''(0)$	$-\theta'(0)$	$-\theta'(0)$
	$fw = 0.1$				$fw = -0.1$			
0°	0.10462	0.14481	0.16572	0.18267	0.06283	0.09302	0.22840	0.24557
30°	0.22380	0.27129	0.19086	0.21952	0.18143	0.21928	0.25543	0.28504
45°	0.28938	0.34058	0.20882	0.24589	0.24666	0.28844	0.27492	0.31355
60°	0.42836	0.48647	0.26151	0.32539	0.38483	0.43402	0.33300	0.40073

Table 7: Values of C_{f_x} and Nu_x with variations in θr and h for the case of suction $fw > 0$ and injection $fw < 0$

		VEC	CEC	VEC	CEC	VEC	CEC	VEC	CEC
		$-f''$	$-f''$	$-\theta'(0)$	$-\theta'(0)$	$-f''$	$-f''$	$-\theta'(0)$	$-\theta'(0)$
θr	h	$fw = 0.1$				$fw = -0.1$			
2.5	0.2	0.19324	0.23874	0.09386	0.11238	0.15827	0.19597	0.14474	0.16381
7.0	0.2	0.18530	0.23035	0.20828	0.23484	0.14117	0.17595	0.27618	0.30349
10.0	0.2	0.18328	0.22806	0.22790	0.25587	0.13773	0.17186	0.29889	0.32767
0.5	0.0	0.22655	0.27859	0.02324	0.04463	0.18683	0.22973	0.07881	0.10063
0.5	0.3	0.16388	0.20481	0.27978	0.30750	0.14557	0.18117	0.24624	0.27165
0.5	0.6	0.05500	0.07371	0.73525	0.78544	0.11966	0.15038	0.35144	0.38006

4.3 Graphs and Discussion

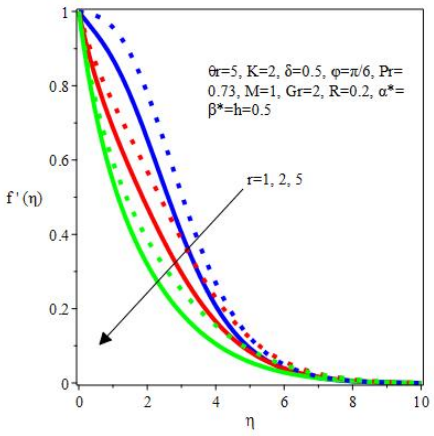

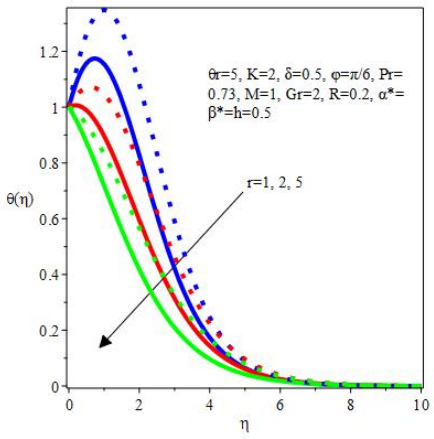

Fig.2. Velocity profiles for r **Fig.3** Temp. profiles for r

Both velocity and temperature profiles decrease with a rise in r for $fw > 0$ and $fw < 0$. The boundary layer structure is thinner in case of suction than injection in both profiles.

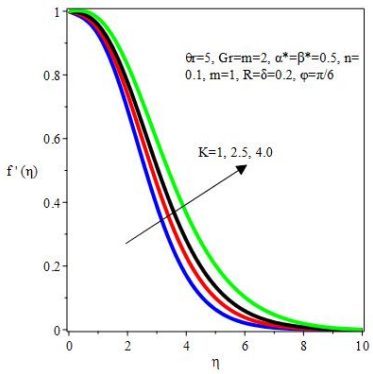

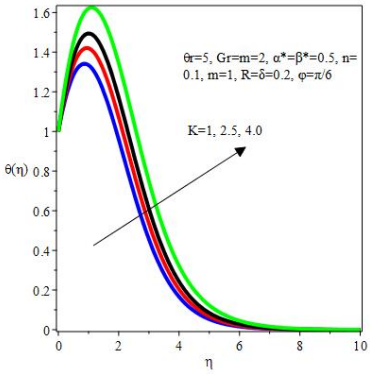

Fig. 4. Velocity profiles for K **Fig. 5** Temp. profiles for K

In figures 4 and 5. It is noticed that a rise in the magnitude of the material parameter K boost both velocity and temperature fields

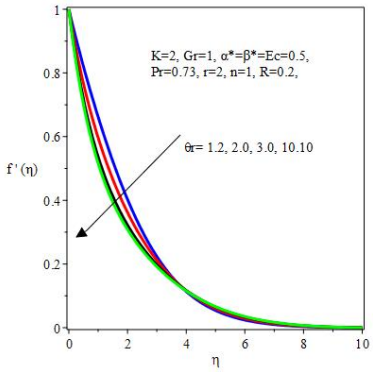

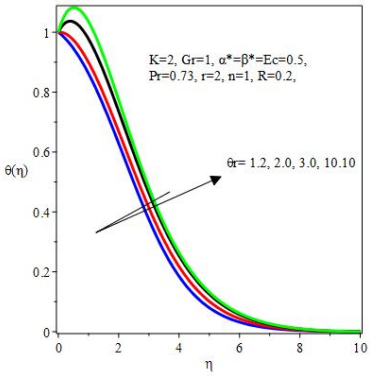

Fig.6. Vel.profiles for $\theta r > 0$ **Fig.7** Temp.profiles for $\theta r > 0$

Figs. 6 and 7 show the effects of $\theta r > 0$ on the velocity distribution and temperature profiles. The graph in figure 6 implies a decrease in the velocity while the temperature advances with a rise in (θr). As the viscosity increase, the fluid motion falls while the thermal field is enhanced.

As $(\theta r \Rightarrow 0)$ the effect becomes negligible.

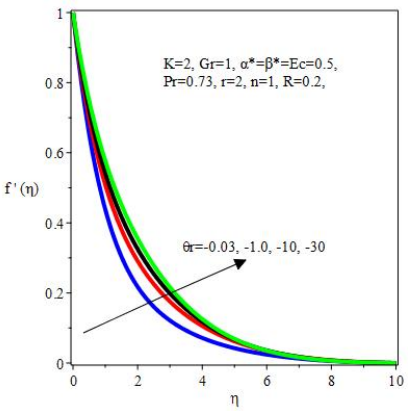

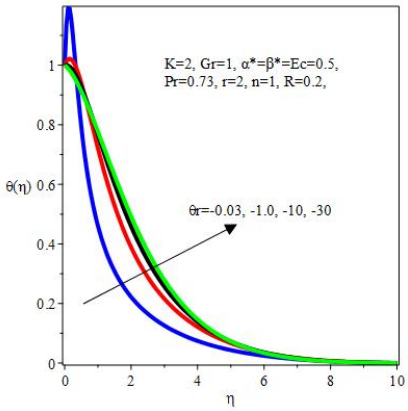

Fig.8 Velocity profiles for $\theta r < 0$ **Fig.9** Temp.profiles for $\theta r < 0$

The graph of the velocity function against η for various values of $\theta r < 0$ is displayed in figure 8. Here, the velocity as well as temperature increases for $\theta r < 0$.

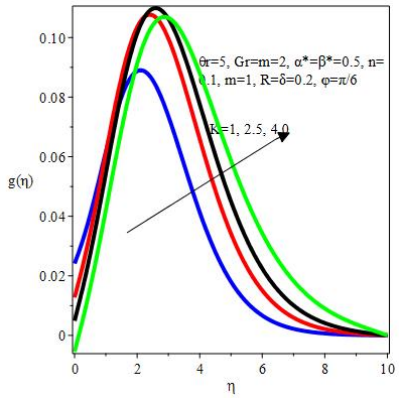

Fig.10. Microrotation profiles for K

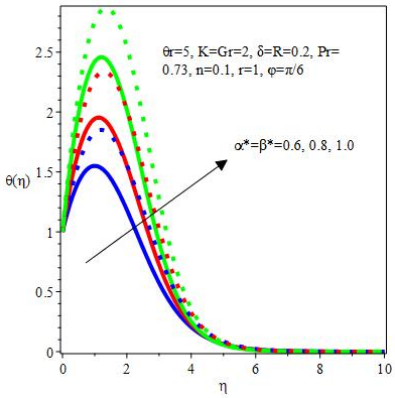

Fig.11. Temp.profiles for $\alpha^\star = \beta^\star$

Figures 10 and 11 show the effects K and $\alpha^\star = \beta^\star$ on the microrotation and temperature profiles respectively. Increase in the material term K enhances microrotation profiles while the thermal boundary layer thickens with rising values of $\alpha^\star = \beta^\star$.

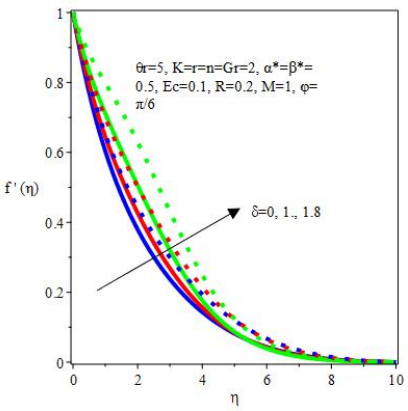

Fig.12. Velocity profiles for δ

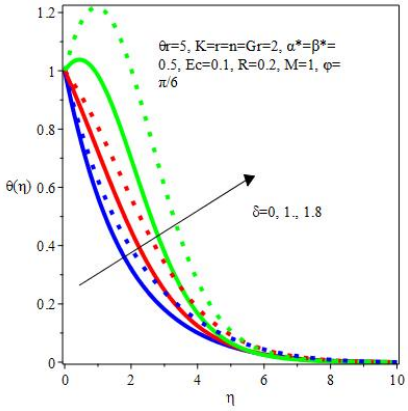

Fig.13 Temperature profiles for δ

Figures 12 and illustrate the effects of δ on the velocity and temperature profiles. It is clearly shown that both boundary layers grow with higher values of δ

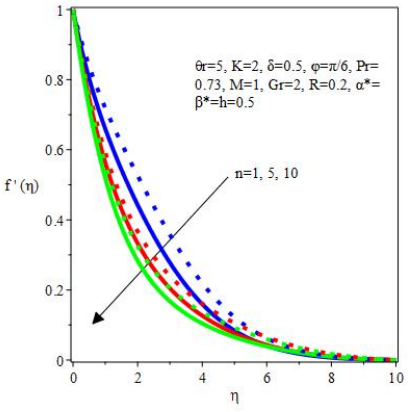

Fig.14. Velocity profiles for n

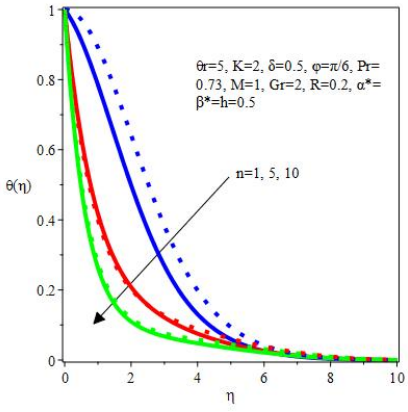

Fig.15 Temp.profiles for n

Figs. 14 and 15 show the effects of n on velocity and temperature profiles. A rise in n dampens both velocity and temperature. The boundary layer thickness thins out for suction in both profiles.

5 Conclusion

This current work studied heat transfer analysis of magneto-micropolar fluid flow passing an inclined nonlinear stretching sheet with variable viscosity, thermal conductivity and electrical conductivity. The influence Joule heating as well as nonuniform heat source/sink, viscous dissipation are also investigated on the thermal field. The controlling modelled equations are converted into dimensionless form by means of similarity

transformation. Thereafter, a numerical approach is adopted to solve the equations. The results in the limiting case compared favourably with the earlier published data in the literature. The following points have been observed from the study:

- VEC offers a better reduction in the viscous shear stress (Cf_x) than the CEC.
- the rate of heat transfer across the surface (Nu_x) is higher for the CEC.
- The (Cf_x) is found to reduce as $K, \theta r, \delta$ increases but rises with φ and r
- The (Nu_x) appreciates with $K, \theta r, \delta$ and φ but falls for r.
- Injection reduces the (Cf_x) while enhancing the (Nu_x).
- Velocity as well as temperature decreases for ($\theta r > 0$).
- Velocity as well as temperature increases for $\theta r < 0$.
- Both velocity & temp. profiles decrease with a rise in r.
- The BLT is thinner in case of suction than injection in both profiles.

References

Ahmad, K. and Ishak, A. and Nazar, R. (2013), Micropolar Fluid Flow and Heat Transfer over a Non-linearly Stretching Plate with Viscous Dissipation. *Mathematical Problems in Engineering*, 2013, 1-5. doi.org/10.1155/2013/257161.

Alinejad, J. and Samarbakhsh, S. (2012), Viscous Flow over nonlinearly Stretching Sheet with Effects of Viscous Dissipation. *Journal of Applied Mathematics*, 1-10.

Akinbobola, T. E., Okoya, S. S. (2015). The flow of second grade fluid over a stretching sheet with variable thermal conductivity and viscosity in the presence of heat source/sink, *Journal of Nigeria Mathematical Society*, 34, 331-342. []Cortell, R. (2008), Effects of Viscous Dissipation and Radiation on the Thermal Boundary Layer Over a nonlinearly Stretching Sheet. *Physics Letter A*,

Das, S., Jana, R. N. and Makinde, O. D. (2015). Magnetohydrodynamic mixed convective slip flow over an inclined porous plate with viscous dissipation and Joule heating. *Alexandria Engineering Journal, 54*, 251-261.

Das, K. and Jana, S. and Kundu, P.K. (2015), Thermophoretic MHD Slip Flow over a permeable surface with variable fluid properties. *Alexandria Engineering Journal*, 35- 44.

Elbashbeshy, E. M. A. (1998). Heat transfer over a stretching surface with variable surface heat flux. *J. Phys. D: Appl. Phys. 31*, 1951-1954.

Eringen, A. C. (1964). Simple microfluids. International Journal of Engineering Science, 2(2), 205-217.

Eringen, A. C. (1966). Theory of micropolar fluids. *J. Math. Anal. Appl., 16*, 1-18.

Eringen, A. C. (1972). Theory of thermo-microfluids. *Journal of Mathematical Analysis and Applications, 38*, 480-496.

Fatunmbi, E. O. and Fenuga, O. J. (2017). MHD micropolar fluid flow over a permeable stretching sheet in the presence of variable viscosity and thermal conductivity with Soret and Dufour effects. *International Journal of Mathematical Analysis and Optimization: Theory and Applications, 2017*, 211- 232.

Hayat, T. and Abbas, Z. and Javed, T. (2008), Mixed convection flow of a micropolar fluid over a non-linearly stretching sheet. *Physic Letter A*, 372, 637 – 647.

Helmy, K. A. (1995). MHD boundary layer equations for power-law fluids with variable electric conductivity, *Meccanica*, 30, 187-200.

Keimanesh, R. and Aghanajafi, C. (2017). Effect of temperature-dependent viscosity and thermal conductivity on micropolar fluid over a stretching sheet. *Tehni?ki Vjesnik, 24*(2), 371-378. doi: 10.17559/TV-20150517072748

Khedr, E. M., Chamkha, A. J. and Bayomi, M. (2009). MHD flow of a micropolar fluid past a stretched permeable surface with heat generation or absorption. *Nonlinear Analysis: Modelling and Control, 14*(1), 27-40.

Kumar, H. (2017). Heat and mass transfer on isothermal inclined porous plate in the presence of chemical reaction. *International Journal of Pure and Applied Mathematics, 113*(5), 523-539. doi: 10.12732/ijpam.v113i5.1

Kumar, L. (2009). Finite element analysis of combined heat and mass transfer in hydromagnetic micropolar flow along a stretching sheet. *Comput Mater Sci, 46*, 841-848. Doi: 10.1371/journal.pone.0059393

Lukaszewicz, G. (1999). *Micropolar fluids: Theory and Applications* (1st Ed.). Birkhauser, Boston.

Mahmoud, M. A. A. (2007). Thermal radiation effects on MHD flow of a micropolar fluid over a stretching surface with variable thermal conductivity *Physica A , 375*, 401-410. doi:10.1016/j.physa.2006.09.010.

Oahimire, J. I. and Olajuwon, B. I. (2013). Hydromagnetic flow near a stagnation point on a stretching sheet with variable thermal conductivity and heat source/sink, *International Journal of Applied Science and Engineering*, 11(3), 331-341.

Rahman, M.M and Uddin, M.J. and Aziz, A. (2009, Effects of variable electric conductivity and non-uniform heat source (or sink) on convective micropolar fluid flow along an inclined flat plate with surface heat flux. *International Journal of Thermal Sciences* 48, 2331 – 2340.

Shamshuddin, M. D. and Thumma, T. (2019). Numerical study of a dissipative micropolar fluid flow past an inclined porous plate with heat source/sink, *Propulsion and Power Research*, 8(1), 56-68.

Salem, A.M. (2013), The Effects of Variable Viscosity, Viscous Dissipation and Chemical Reaction and Heat and Mass Transfer of Flow of MHD Micropolar Fluid along a Permeable Stretching Sheet in a Non-Darcian Porous Medium. *Mathematical Problems in Engineering*, 2013,1-10. doi.org/10.1155/2013/185074 ResearchHindawi Publishing Corporation, 1-10.

Tripathy, R.S. and Dash, G.C. and Mishra, S.R. and Hoque M.M, (2016), Numerical Analysis of hydromagnetic micropolar fluid along a stretching sheet embedded in porous medium with non-uniform heat source and chemical reaction. *Engineering Science and Technology, an International Journal* 19, 1573 – 1581.